

# A Spatially Extended Stochastic Model of the Bacterial Chemotaxis Signalling Pathway

Thomas S. Shimizu\*, Sergej V. Aksenov and Dennis Bray

Department of Zoology  
University of Cambridge  
Downing Street, Cambridge  
CB2 3EJ, UK

We have combined two distinct but related stochastic approaches to model the *Escherichia coli* chemotaxis pathway. Reactions involving cytosolic components of the pathway were assumed to obey the laws of conventional stochastic chemical kinetics, while the clustered membrane receptors were represented in two-dimensional arrays similar to the Ising model. Receptors were assumed to flip between an active and an inactive state with probabilities dependent upon three energy inputs: ligand binding, methylation level due to adaptation, and the activity of neighbouring receptors. Examination of models with different lattice size and geometry showed that the sensitivity to stimuli increases with lattice size and the nearest-neighbour coupling strength up to a critical point, but this amplification was also accompanied by a proportional increase in steady-state noise. Multiple methylation of receptors resulted in diminished signal-to-noise ratio, but showed improved stability to variation in the coupling strength and increased gain. Under the best conditions the simulated output of a coupled lattice of receptors closely matched the time-course and amplitude found experimentally in living bacteria. The model also has some of the properties of a cellular automaton and shows an unexpected emergence of spatial patterns of methylation within the receptor lattice.

© 2003 Elsevier Science Ltd. All rights reserved

**Keywords:** bacterial chemotaxis; sensitivity amplification; cluster of receptors; Ising model

\*Corresponding author

## Introduction

The receptors for peptide hormones, odorant molecules, extracellular matrix molecules, neurotransmitters, major histocompatibility complexes, and chemoeffectors are transmembrane proteins that associate, on their cytoplasmic domains, with intracellular enzymes such as GTP-binding proteins and protein kinases. Signals from outside the cell travel across the plasma membrane to the cytoplasm by means of concerted conformational and chemical changes between the receptors and their associated proteins. In many cases the receptors, with their adjunct proteins, have been found to associate laterally into extended two-

dimensional aggregates in the membrane.<sup>1–5</sup> In such situations interactions are possible between neighbouring receptors so that the lattice as a whole could have properties greater than the sum of its individual parts.

One of the best characterised clusters of membrane receptors is that responsible for chemotaxis in coliform bacteria.<sup>6,7</sup> Aggregates of transmembrane receptors, usually localised at one end of the bacterium, mediate detection of a range of attractants and repellents. Individual receptors have ligand binding domains in the periplasm, and interact with the histidine kinase CheA on the cytosolic side of the plasma membrane. Conformational changes occurring within the receptor, and modulated by the binding of ligands, regulate the activity of the kinase and thereby change the phosphorylation level of the signalling molecule CheY (CheY ~ P). The latter diffuses through the cytoplasm to the flagellar motors where it increases the probability of a change in the direction of flagellar motor rotation. Following a rapid response to attractant, receptors undergo a slower change, due to methylation, which allows the bacterium to adapt to the stimulus. Recent evidence suggests that

Present address: T. S. Shimizu, Laboratory for Bioinformatics, Institute for Advanced Biosciences, Keio University, Fujisawa, 252-8520, Japan.

Abbreviations used: CheY ~ P, phosphorylated CheY protein; FRET, fluorescence resonance energy transfer; SNR, signal-to-noise ratio; *mb*, motor bias; MeAsp,  $\alpha$ -methyl-D-aspartate.

E-mail address of the corresponding author: tom@sfc.keio.ac.jp

cross-talk occurs between groups of neighbouring receptors<sup>8,9</sup> and it has been suggested that nearest-neighbour conformational interactions could explain the very large amplification of signal produced by these receptors.<sup>10</sup>

In the past, two distinct stochastic approaches have been taken to simulate the population of *Escherichia coli* chemotaxis receptors. The first employs a program called StochSim to represent the molecular details of individual receptors, including degree of methylation, conformational state, association with methylation and demethylation enzymes and the state of activity of the associated CheA.<sup>11</sup> This method of simulation is able to reproduce much of the response of swimming *E. coli* to the attractant aspartate, but has so far failed to predict the impressive sensitivity, or gain, of the system. A second approach, developed specifically to address the issue of gain, represents receptors as individual elements in a two-dimensional lattice analogous to the Ising model.<sup>12,13</sup> Although this model is highly simplified and omits many of the molecular details of the chemotactic machinery, it is able to show that a coupled lattice of receptors has the capacity to greatly amplify signals and respond over a wide range of stimulus concentrations.

Here we have combined these two computational approaches. A spatial component has been added to the original StochSim simulation making it possible to represent the positions of individual receptors within a cluster (although the free diffusion of molecules within the cytoplasm is not represented). This new framework allows interactions between neighbouring receptors to be explored while retaining the molecular detail of the StochSim model. The resulting program shows greatly improved chemotactic gain and agrees well with several available experimentally observed results. It also raises the possibility that patterns of receptor methylation could emerge in the lattice as a consequence of the allosteric coupling mechanism.

## Results

### Characterisation of the receptor lattice

#### Calculation of “optimal” coupling

A crucial feature of our computational model is that the conformational state of each receptor is sensitive to the conformational states of its nearest neighbours. The strength of this “conformational coupling”, measured by the free energy term  $E_j$  (see Methods and Calculations), has a profound influence on the performance of the lattice and hence the physiological response of the bacterium. Presumably, if our model is correct, this value would have been tuned by evolution in order to optimise information processing by the receptor clusters.

In the previously described model of the chemotaxis receptor lattice by Duke & Bray,<sup>13</sup> the strength

of nearest-neighbour interactions attains its optimal value as it approaches the critical coupling energy of an analogous Ising model. This is a well-defined quantity that can be calculated analytically from first principles, and the correlation distance (a measure of how far conformations can spread) grows following a power law as the coupling energy approaches the critical point. The essence of the Duke & Bray approach is to leverage this sharp increase to obtain an amplification in signal upon ligand binding, which is done by setting the coupling parameter very close to, but just below the critical point. Because the response of the Ising lattice to fluctuations and perturbations is proportional to the square of the correlation length, significant amplification can be achieved by tuning the coupling parameter appropriately. A more subtle, but equally important, requirement for this mechanism to work as an effective amplifier is to ensure that the global behaviour of the modelled lattice, given an appropriate coupling parameter, will actually resemble an Ising lattice. In the Duke & Bray model, this is achieved by the way in which its receptors are modelled. Specifically, both the “virgin” receptor (ligand unbound and unmethylated), and “adapted” receptor (ligand bound and methylated) are set to have unbiased activity states (i.e. the free energy change upon activation is zero). Most receptors will be in one of these two states when the cluster is adapted, so the significant free-energy contributions at steady state arise primarily from thermal fluctuations and nearest-neighbour interactions: precisely the two factors that determine the critical behaviour in the classical Ising model.<sup>14</sup> Although it omits molecular details of the chemotaxis network for the sake of simplicity, this model demonstrates that amplification can be achieved through a simple spatial interaction mechanism.

In reality, however, bacterial chemoreceptors have multiple methylation sites that increase the heterogeneity in the free energy of the population and thus introduce additional noise into the system. In broad terms we found that the StochSim model with four methylation sites behaves similarly to its variant with one site at extreme values of  $E_j$ . If  $E_j$  is very low, the performance of the lattice is indistinguishable from that of an uncoupled system, whereas if  $E_j$  is very high, the system behaves in an all-or-none fashion and will not respond to input stimuli. This is shown in [Figure 1](#) for a square lattice with 4225 receptors stimulated with a step increase of 0.1  $\mu\text{M}$  aspartate for zero and  $-3.06 \text{ kcal mol}^{-1}$  coupling energy. But between these extreme behaviours, the level of steady-state noise (fluctuations in total receptor activity) increases gradually with coupling energy until it segues into an oscillatory all-or-none behaviour. As a result, a single value of  $E_j$  that discriminates between signal-enhancement behaviour and all-or-none behaviour does not exist, and we must use empirical methods to select an optimal value.

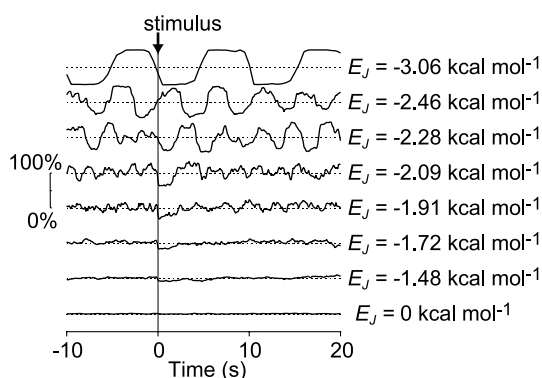


**Figure 1.** Effect of changing the coupling energy. A square lattice with 4225 receptors, four methylation sites per receptor and periodic boundaries, was stimulated by a step increase of  $0.1 \mu\text{M}$  aspartate at time 0 (fine vertical line) at different values of coupling energy  $E_J$ . The coupling energy used is shown beside each trace. Horizontal lines indicate the mean steady-state level of activity. The vertical scale shows percentage of total active receptors. Note that there is not a single sharp threshold of  $E_J$  but rather a broad range of values, over which signal responses change gradually. At  $E_J = 0.0$ , the behaviour of the receptor cluster is that of an uncoupled system with the same number of receptors. Because of the low gain of the uncoupled lattice, the small aspartate stimulus is not detected. Very high value of  $E_J = -3.06 \text{ kcal mol}^{-1}$  results in spontaneous, all-or-none “flipping” behaviour that masks the attractant response.

For the purpose of illustrating this procedure, let us first present a simplified StochSim model. This model is similar to the Duke & Bray model in that receptors with only one methylation site are arranged in an interacting cluster. In contrast to the Duke & Bray model, however, it explicitly represents the downstream components of the pathway (CheY, CheR and CheB) and their interactions with the receptor complex (as in the previously described StochSim model<sup>11</sup>). We found that this more realistic representation of reactions in the one-methylation-site model complicates the selection of parameters related to the adaptation process. This model would not adapt exactly with parameters taken from either the Duke & Bray or StochSim models, but we found that near-exact adaptation could be obtained with carefully chosen parameters (see Appendix A). The requirements for near-exact adaptation include setting both the methylated and unmethylated receptors to have highly biased activities, which in turn results in a smaller response and hence a higher threshold of signal detection (see Appendix A).

To choose an optimal value for  $E_J$ , we studied how the output signal-to-noise ratio (SNR) and the signal gain depend on  $E_J$ . We computed these quantities from simulations in which the magnitude of the aspartate step stimulus was  $1 \mu\text{M}$  and  $0.1 \mu\text{M}$  for the one- and four-methylation-site models, respectively, just above their respective

thresholds of detection.<sup>†</sup> Figure 2(a) shows that the output SNR for total receptor activity in the lattice varies over a considerable range of coupling energies. We found that the one-methylation-site model requires a higher value of  $E_J$  ( $-2.71 \text{ kcal mol}^{-1}$ ) than the four-methylation-site model ( $-1.71 \text{ kcal mol}^{-1}$ ) to reach its SNR maximum (Table 1). This offset is in contrast to the Duke and Bray model, whose critical point occurs at a much lower value of  $E_J$  ( $\sim 0.3 \text{ kcal mol}^{-1}$ ) than in the four-methylation-site model, and is another consequence of the highly biased conformational states of receptors. Noise in the lattice increases with coupling energy, regardless of the number of methylation sites (data not shown), but we found that the value of the SNR at maximum is higher for the one-methylation-site model. The relationship between the SNR and coupling energy is analogous to that between SNR and noise intensity in the phenomenon of intrinsic stochastic resonance (as seen, for example, in a coupled neuronal system<sup>15</sup>). Increasing internal noise in the lattice does not lead to a monotonic decrease in the efficiency of signal detection, rather, there exists some optimal coupling strength at which signal enhancement reaches a maximum, and above which the enhancement tapers off gradually. The overall shapes of the SNR and gain curves remain unchanged when the magnitude of the aspartate stimulus is varied (data not shown). The value of the SNR at maximum increases with stimulus size, while the maximum gain decreases.

As Figure 2(a) shows, the model with four methylation sites has a broader SNR maximum than the model with one site, and is thus more stable to variations in  $E_J$ . Stability is of interest here not only on general grounds of robustness, but also because the signal gain continues to increase with  $E_J$  beyond the SNR maximum (Figure 2(b)). When SNR is maximised, the one-methylation-site model consistently gives weaker signal amplification with a gain of  $\sim 3.8$  compared to  $\sim 15$  for the four-methylation-site model (Table 1). We chose the coupling strength of  $-1.91 \text{ kcal mol}^{-1}$  as the optimal value to be used in all simulations with the square lattice with four methylation sites, because this coupling energy gives the maximal gain achievable without crossing over to the critical oscillatory behaviour, even though the SNR is slightly suboptimal.<sup>‡</sup> (Figure 2(a) and (b) and Table 1).

<sup>†</sup> We determined thresholds by comparing the maximum response size for a given aspartate stimulation with the standard deviation of the steady-state fluctuations in the absence of stimulus at zero coupling (data not shown).

<sup>‡</sup> It should be noted that this choice of maximising gain at the cost of a slight reduction in SNR is arbitrary. Because the flagellar motor is likely to possess properties that will filter out some fluctuations in CheY  $\sim$  P levels (see Discussion), we feel that this choice is justified. However, it is of course entirely possible that the actual costs and benefits for a living bacterium would favour maximising SNR.

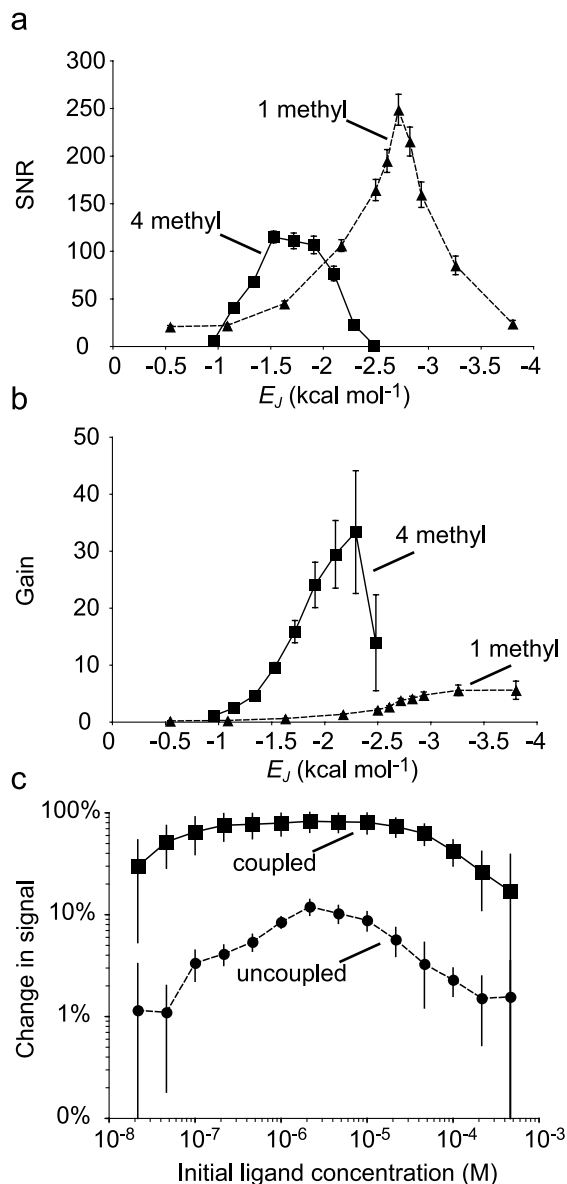


**Figure 2.** Effect of coupling energy on signal enhancement. A square lattice with 4225 receptors and periodic boundaries was stimulated by a step increase of aspartate. (a) Output SNR in total activity of the lattice. (b) Gain in total activity of the lattice. (c) Comparison of coupled and uncoupled models with four methylation sites. Continuous lines and squares indicate model with four methylation sites, broken lines and triangles indicate the model with one methylation site, and broken lines and circles indicate the uncoupled model with four methylation sites. In (a) and (b), the lattice was stimulated with 0.1  $\mu$ M (model with four methylation sites) and 1  $\mu$ M (model with one methylation site) aspartate added to zero background. In (c), the lattice was subjected to a doubling of an initial ambient concentration of aspartate. The horizontal axis shows the size of the initial stimulus. The response here is measured as the fractional change in receptor activity. It can be seen that the signal is amplified in the coupled model over the uncoupled model throughout the entire range of ambient concentrations tested. Error bars show the steady-state level of noise in the system, which can mask the signal at the low and high extremes of ambient concentration.

We have also found that the range of response is enhanced by conformational coupling. The effect of receptor coupling on the amplitude of an attractant response was examined by running a series of simulations in which a lattice was first allowed to adapt to varying concentrations of aspartate, and then subjected to a doubling of this concentration (Figure 2(c)). It can be seen that coupling has a major effect on the size of the response over the entire range of ambient concentrations. In both the coupled and the uncoupled case the response is masked by the steady-state noise at high and low extremes of ambient concentration. If we interpret the range over which the signal is not masked as the effective dynamic range of the system, then the coupling mechanism extends this range by an order of magnitude. The range of response is also larger in the model with four methylation sites than in the model with one site (data not shown).

#### Effects of lattice size and geometry

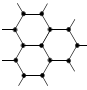
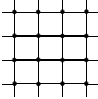
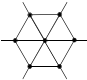
In order to investigate the effects of lattice size and geometry on the signalling properties of the response, simulations were performed with receptors with four methylation sites arranged in hexagonal, square, and trigonal arrays with sizes ranging from 4 to 4225 receptors as described in Methods and Calculations.

Optimal coupling energies for hexagonal and trigonal lattices were estimated in a similar way to that described above for a square geometry. Those values that maximise SNR are listed in Table 1 together with the corresponding SNR and gain that they yield. It is interesting to compare these energy values to those computed for standard Ising lattices. The latter are usually computed assuming a periodic lattice in the absence of any external field, so as noted above, the only parameters required for these calculations are the number of nearest neighbours and temperature. In the StochSim model, methylation and ligand binding provide additional energy to the system, but one might expect conservation in the ratio of characteristic coupling energies (e.g. those maximising SNR) between the different geometries. Critical energies in the Ising model at  $T = 310$  K are  $-1.62$ ,  $-1.09$ , and  $-0.68$ † kcal mol<sup>-1</sup> for hexagonal, square, and trigonal lattices, respectively.<sup>14</sup> Ratios are 1.49 and 1.60 for hexagonal:square and square:trigonal geometries, respectively. The energy values that maximise SNR (Table 1) give the ratios of 1.50 for hexagonal:square and 1.44 for square:trigonal, geometries, respectively, which is very close to expected ratios.

Increasing the number of nearest neighbours (that is, going from hexagonal to square to trigonal geometry) decreases SNR, but increases gain (Table 1). This can be understood by observing that the

† These values are four times the critical interaction energy in the Ising model (see Appendix B).

**Table 1.** Optimal and maximising coupling energies  $E_j$  and corresponding values of SNR and gain for receptor activity, for receptor lattices with different sizes and geometries

Lattice geometry	Size	Boundary condition	$E_j$ (kcal mol <sup>-1</sup> )	SNR	Gain	Illustration
Hexagonal	4224	Periodic	-2.57 <sup>a</sup>	154 ± 7	15 ± 2	
Square	4224	Periodic	-1.71 <sup>a</sup>	111 ± 8	16 ± 2	
Square	4225	Periodic	-2.71 <sup>a,b</sup>	248 ± 16	3.8 ± 0.3	
Trigonal	4224	Periodic	-1.19 <sup>a</sup>	126 ± 9	25 ± 4	
Square	4224	Periodic	-1.91 <sup>c</sup>	107 ± 9	24 ± 4	
Square	625	Periodic	-1.91 <sup>c</sup>	119 ± 11	27 ± 5	
Square	625	Finite	-1.91 <sup>c</sup>	109 ± 9	16 ± 2	
Square	25	Periodic	-1.91 <sup>c</sup>	48 ± 4	5.8 ± 0.6	
Square	25	Finite	-1.91 <sup>c</sup>	34 ± 2	3.3 ± 0.3	

Lattice geometries used in the simulations are shown to the right. The circles indicate the location of the receptors and the straight lines the interactions. The concentration of aspartate was 0.1 μM for the model with four methylation sites and 1 μM for the model with one site.

<sup>a</sup> Coupling energy that maximises SNR.

<sup>b</sup> Model with one methylation site.

<sup>c</sup> Optimal coupling energy (see the text).

noise in the lattice increases with the number of nearest neighbours, and that gain is strongly correlated with noise. For smaller lattices, the effect of boundaries becomes more pronounced and both SNR and gain become lower.

In the remainder of this article, we have chosen the square lattice as a reference for comparison with experimental data. Although the gain at optimal coupling energies is comparable between different geometries, a square lattice provides more stability against variation in coupling energy  $E_j$ . In fact, a higher gain for the square lattice can be obtained without compromising SNR.

### Comparison with experiment

Although they are based on simple geometric lattices, the receptor clusters we have modelled have a complex and rapidly changing molecular composition due to ligand binding, conformational changes and methylation. The range of their responses to different stimuli is also broad and provides a basis for detailed comparison with experimental records. For this part of the work, we selected a square lattice with periodic boundaries containing 4225 receptors, each with four methylation sites.

### Response to a pulse of attractant

One of the most revealing tests is the application of a brief pulse of stimulus (aspartate), which provides a succinct phenomenological description of the system's kinetic characteristics. Experimentally,

it has been shown that the cumulative average response of *E. coli* cells to a short pulse (ca 0.1 second) of aspartate is biphasic.<sup>16</sup> The first phase of the response lasts for approximately one second, over the course of which motor bias rapidly jumps to a peak value and then falls below, or undershoots, the steady-state bias. The second phase of the response is a slower recovery to the baseline, which lasts approximately three seconds (Figure 3(a)). The basis of the undershoot can be explained by the negative feedback through the methylation and demethylation reactions. The brief drop in receptor activity during the first phase of the response causes a transient decrease in the catalytic activity of CheB. This results in a small but significant net increase in the total methylation level of the receptor population, which returns to its steady-state level on a slower time-scale.

Because, in the Segall *et al.* experiment,<sup>16</sup> attractant was administered by iontophoretic release from a micropipette at some distance from the target cell, the exact amplitude of the aspartate pulses was not precisely known. However, indirect calculations based on the duration of adaptation suggest that the pulse in Figure 3(a) raised the receptor occupancy by 0.19 for 0.02 second.<sup>16</sup> In the uncoupled simulation (Figure 3(b)), the first of the two phases could be reproduced provided a sufficiently large pulse of aspartate was applied, but no undershoot could be detected, even in response to a pulse of saturating concentration. To account for this lack of feedback gain in the uncoupled system, it is necessary to increase the

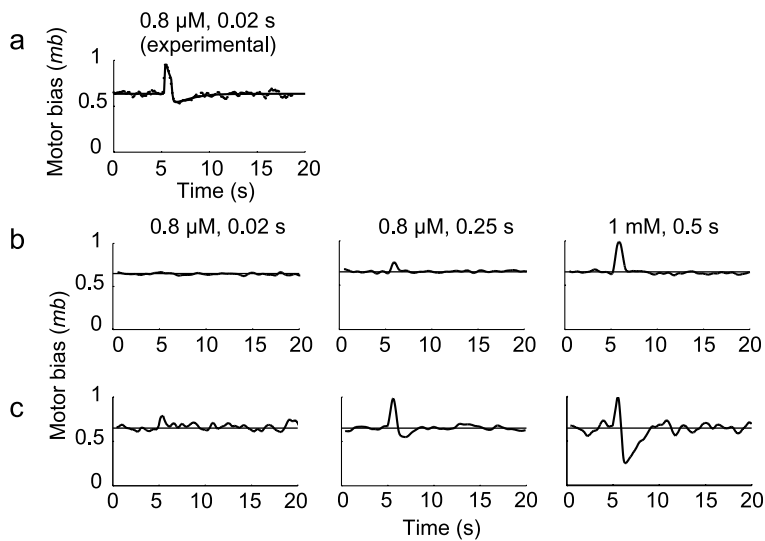


**Figure 3.** Experimental and simulated impulse responses. All panels show the response in motor bias to a brief pulse of aspartate at five seconds. (a) Experimentally observed response to a brief pulse of attractant administered by iontophoretic release (exposure to  $0.8 \mu\text{M}$  aspartate for 0.02 second).<sup>16</sup> (b) Response of the uncoupled model ( $E_I = 0.0$ ). (c) Improved response of the present model with optimal coupling energy ( $E_I = -1.91 \text{ kcal mol}^{-1}$ ). In (b) and (c), motor bias was calculated using equation (4).

methylation and demethylation rates nearly 100-fold (data not shown). Similar results are obtained in a differential equation-based deterministic model of chemotaxis (M. D. Levin, personal communication†). By contrast, in a lattice with optimal coupling (Figure 3(c)), the simulation produces a significant undershoot of comparable size and duration to the experimentally determined response with values of the methylation and demethylation reactions very close to experimentally reported values (see Methods and Calculations).

The fact that the undershoot depends on the presence of coupling in our model reflects the fact that the coupling mechanism works to amplify the effect of methylation as well as ligand binding. The effect of the small increase of net methylation on total activity is insufficient to produce an undershoot in the uncoupled model (Figure 3(b)), but a similar increase in the coupled model affects many more receptors due to the spread of conformations in the lattice and produces an undershoot of comparable magnitude to the experimentally observed impulse response (Figure 3(a) and (c)).

### Dose-response

The amplitude, or gain, of the chemotactic response has been measured in two recent studies. In the first, fluorescence resonance energy transfer (FRET) was employed to estimate the *in vivo* concentration of CheY ~ P following stepwise increments of attractant.<sup>17</sup> Although the measurements were made by stimulating cells with  $\alpha$ -methyl-D-aspartate (MeAsp), the non-metabolisable analogue of aspartate with lower binding affinity for Tar, the results can be compared with

our simulations by converting the stimulus size to an aspartate concentration that would give an equivalent receptor occupancy (see Methods and Calculations).

This comparison, shown in Figure 4, reveals that our best simulation conditions (square lattice with 4225 receptors and optimal coupling energy  $E_I = -1.91 \text{ kcal mol}^{-1}$ ) fall some way short of the observed response. The receptor occupancy required to achieve a half-maximal decrease in CheY ~ P concentration in the computer model is 0.036, whereas that of the real bacterium is close to 0.01. The shape of the two curves is also distinct, since the simulated curve does not fit a sigmoid in equation (5) at smaller step sizes  $< 0.02 c_{0.5}$ , where  $c_{0.5} = \sqrt{K_d^a K_d^i}$  is the concentration that gives 50% occupancy (in other words, CheY ~ P response is more sensitive than is predicted by positive cooperativity). Also, our simulated curves tend to a non-zero baseline for very high step sizes, so that even at saturating aspartate, the initial response in CheY ~ P concentration does not reach zero. This is due to a certain fraction of receptors having a non-zero probability of being active, even in the ligand-bound state (Table 2). This fraction is highest in the uncoupled model and decreases with higher coupling energies, which favour progressive inactivation of neighbouring receptors. Experimental data were obtained with wild-type cells containing both major chemoreceptors, Tsr and Tar, and the interactions between the two types of receptors might influence the response, contributing to the discrepancy between experiment and simulation, which was done for receptor Tar only. Despite these discrepancies it is clear that the coupled lattice is much closer to reality than the uncoupled lattice, which requires an almost 30-fold greater concentration of aspartate to achieve half-maximal CheA inhibition. Figure 4 also shows results of simulations with square lattices each with 25 receptors,

† BCT, the deterministic simulator of bacterial chemotaxis is available for download from <http://www.zoo.cam.ac.uk/comp-cell/>

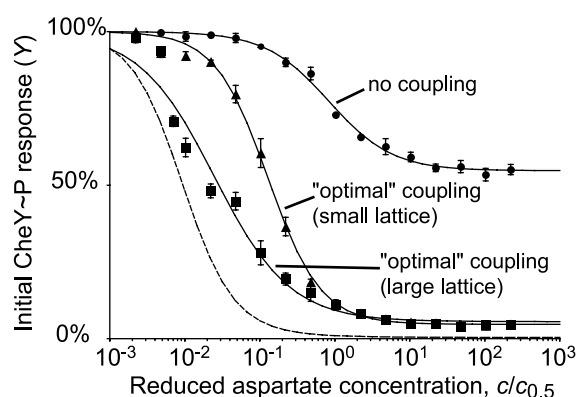


**Figure 4.** Response to step stimuli of aspartate at zero background concentration measured as percent change in CheY ~ P concentration  $Y$  (see Methods and Calculations). Response is calculated for square lattices with zero coupling ( $E_j = 0.0$ , circles) and optimal coupling ( $E_j = -1.91 \text{ kcal mol}^{-1}$ ) with 25 receptors per cluster (triangles) and 4225 receptors per cluster (squares). Continuous lines indicate least-squares fit to sigmoid in equation (5) with parameters  $b = 0.047(\pm 0.007)$ ,  $EC_{50} = 0.58 \mu\text{M}$  (95% confidence interval from  $0.26 \mu\text{M}$  to  $1.3 \mu\text{M}$ ),  $h = 1.23(\pm 0.06)$  (25 receptors per cluster),  $b = 0.06(\pm 0.02)$ ,  $EC_{50} = 0.11 \mu\text{M}$  (95% confidence interval from  $0.046 \mu\text{M}$  to  $0.27 \mu\text{M}$ ),  $h = 0.87(\pm 0.09)$  (4225 receptors per cluster, optimal coupling), and  $b = 0.547(\pm 0.006)$ ,  $EC_{50} = 3.8 \mu\text{M}$  (95% confidence interval from  $1.6 \mu\text{M}$  to  $8.7 \mu\text{M}$ ),  $h = 1.03(\pm 0.06)$  (4225 receptors per cluster, zero coupling). Broken line represents equation (7) fitted by Sourjik & Berg<sup>17</sup> to changes in intracellular CheY ~ P concentration measured as the FRET signal of association of CheY ~ P and CheZ in response to step addition of MeAsp. For comparison, we converted MeAsp concentration to that of aspartate that would give an equivalent receptor occupancy (converted  $EC_{50} = 43 \text{ nM}$ , see Methods and Calculations).

which occupies an intermediate position between uncoupled curve and coupled curve with 4225 receptors per lattice.

The same simulations compare more favourably to the results of a second study, in which swimming bacteria were exposed to a sudden increment of attractant, released by flash photolysis<sup>18</sup> (Figure 5). In this case the response to attractant was measured by the changes in swimming behaviour monitored by video analysis. The performance of the coupled and uncoupled computer models can be compared to the observed swimming behaviour by converting the changes in CheY ~ P concentration into changes in motor bias  $\Delta mb$  using equation (4). Figure 5(a) shows the result of this conversion plotted as a function of the change in receptor occupancy  $\Delta occ$ . Neither the shape of the reported logarithmic relation curve nor the sensitivity (the step-size required for a half-maximal response) can be reproduced by the uncoupled model (Figure 5(a), circles), despite the fact that a Hill coefficient as high as  $n_H = 10.3^{19}$  was used for the conversion. This confirms that high cooperativity at the motor alone is insufficient to explain the observed sensitivity. Incorporation of the coupling mechanism (Figure 5(a), squares), however, brings the point of half-maximal response very close to the experimentally observed relation (Figure 5(a), broken curve).

It may be noted however that the logarithmic form is still not reproduced. The slope of the coupled model's response curve is steeper than the observed relation. The simulated curve rises rapidly to saturation, reaching maximal bias at only 2% receptor occupancy, whereas saturation with caged attractant required 18%.<sup>18</sup> A more

**Table 2.** Values of activation probabilities ( $p$ ) and difference between the free energy of the active and inactive states ( $\Delta G$ ,  $\text{kcal mol}^{-1}$ ) for receptors in different states of methylation, ligand binding, and different number of active nearest neighbours for the square lattice

		Ligand unbound							Ligand bound				
		active neighbours							active neighbours				
	Species	0	1	2	3	4	Species	0	1	2	3	4	
$p$		0.00	0.00	0.02	0.45	0.97		0.00	0.00	0.00	0.11	0.83	
$\Delta G$		6.99	4.70	2.41	0.12	-2.18		8.19	5.90	3.61	1.32	-0.97	
$p$		0.00	0.00	0.12	0.85	1.00		0.00	0.00	0.02	0.45	0.97	
$\Delta G$		5.79	3.50	1.20	-1.09	-3.38		6.99	4.70	2.41	0.12	-2.18	
$p$		0.00	0.02	0.50	0.98	1.00		0.00	0.00	0.12	0.85	1.00	
$\Delta G$		4.58	2.29	0.00	-2.29	-4.58		5.79	3.50	1.20	-1.09	-3.38	
$p$		0.00	0.15	0.88	1.00	1.00		0.00	0.02	0.50	0.98	1.00	
$\Delta G$		3.38	1.09	-1.20	-3.50	-5.79		4.58	2.29	0.00	-2.29	-4.58	
$p$		0.17	0.89	1.00	1.00	1.00		0.03	0.55	0.98	1.00	1.00	
$\Delta G$		0.97	-1.32	-3.61	-5.90	-8.19		2.18	-0.12	-2.41	-4.70	-6.99	

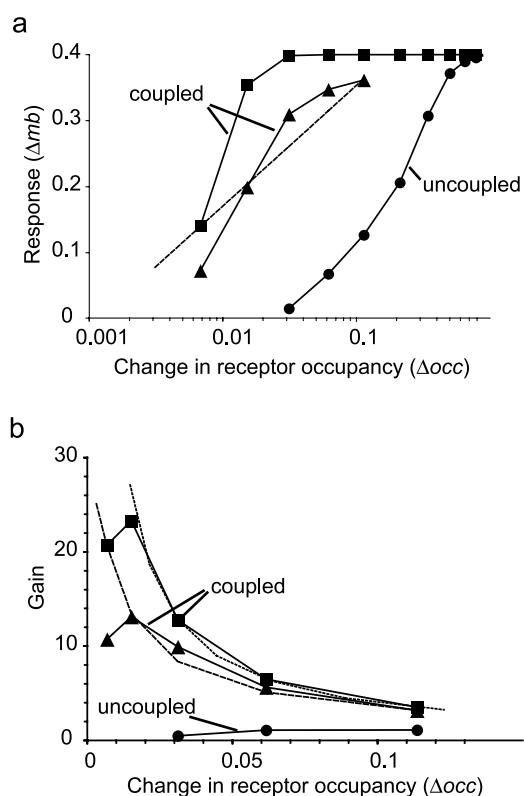


**Figure 5.** Swimming response of *E. coli* measured as change in motor bias  $\Delta mb$  and gain as a function of change in receptor occupancy. Comparison of simulated results with square lattice with 4225 receptors to the experimental data of Jasuja *et al.*<sup>18</sup> (a) Simulation of  $\Delta mb$  by the uncoupled (circles) and coupled (optimal coupling energy  $-1.91 \text{ kcal mol}^{-1}$ , squares) model compared to the observed logarithmic relation (broken curve). A steady-state motor bias of 0.6 was assumed, so the maximum possible  $\Delta mb$  here is 0.4. Triangles are the response predicted for a system with 38.25% of the receptors in clusters (see the text). Motor bias was computed from simulated  $\text{CheY} \sim \text{P}$  concentration using a Hill-type relation in equation (4). (b) Observed and simulated gain for motor bias of the pathway. Dotted line shows the maximum achievable gain (i.e. the gain required to obtain a  $\Delta mb$  of 0.4). Other symbols and curves are as in (a). Note that data only for small concentration jumps are plotted in (b) because the response in motor bias saturates at higher levels.

graded response, closer to the observed relation, can be obtained if it is assumed that only a certain fraction of the total receptor population is clustered. The response of the whole system then resembles a weighted average of the coupled and uncoupled responses (Figure 5(a), triangles), with a slope much closer to the observed logarithmic relation. Standard errors for motor bias measurements in the Jasuja *et al.* data<sup>18</sup> were rather large, around 20%, so quantitative comparison is probably not meaningful.

The gain for each step size can be calculated from  $\Delta mb$  and is shown in Figure 5(b) with the same symbols as in Figure 5(a). Our results agree

qualitatively with the observation that higher gain is achieved for smaller step sizes, a result that is not predicted by the uncoupled model. There is still a difference in the threshold of detection.

### Methylation patterns

The model that we have developed of the lattice of chemotactic receptors has some of the properties of a cellular automaton in that its behaviour is specified by local interactions between neighbouring receptors (even though these interactions are probabilistic in nature). Consequently we might expect that, as with other cellular automata, spatial patterns could emerge in the clustered receptors. With this possibility in mind, we examined the output of the simulations for any regular features in the steady-state levels of methylation (Figure 6(a) and (b)). Composite greyscale images highlighting the distribution of methylation states in the lattice, generated as described in Methods and Calculations, reveal that the two extreme methylation states tend to cluster together in the coupled array (Figure 6(b) and (c)). We also observed that lattices with finite boundaries had an excess of higher methylation states along their edges (Figure 6(d)).

The fraction of receptors in each of the five possible methylation states at equilibrium (in the absence of ligand) is different in the coupled and uncoupled systems (Figure 6(e)). In broad terms, it was found that the proportion of receptor with zero or four methyl groups increases with the strength of coupling. This is compensated mainly by a proportional decrease in the number of receptors with two methyl groups. The number of receptors with one or three methyl groups was nearly constant over the entire range of  $E_j$  values tested.

A striking difference between the coupled and uncoupled models can be found in the relationship between the population-wide average number of methyl groups per receptor and the concentration of  $\text{CheY} \sim \text{P}$ . When the temporal transitions in these quantities are smoothed with a moving average filter (window = ten seconds) to remove rapid fluctuations, there is a linear relationship between methylation level and  $\text{CheY} \sim \text{P}$  concentration (Figure 6(f)). However, there is a dramatic difference in the slopes ( $\sim 60$ -fold) of the coupled and uncoupled data reflecting the effect of coupling on both amplification and feedback. The greater scatter of the data points of the coupled model along the  $\text{CheY} \sim \text{P}$  axis is expected from the higher level of steady-state noise in the system discussed above. However, more interestingly, fluctuations in the average methylation state are much smaller in the coupled system, despite the fact that the higher noise must also cause the variation in  $\text{CheB}$  activity to increase. This rather counter-intuitive result can be understood by observing that receptor-receptor coupling in effect buffers the system against large changes in methylation.

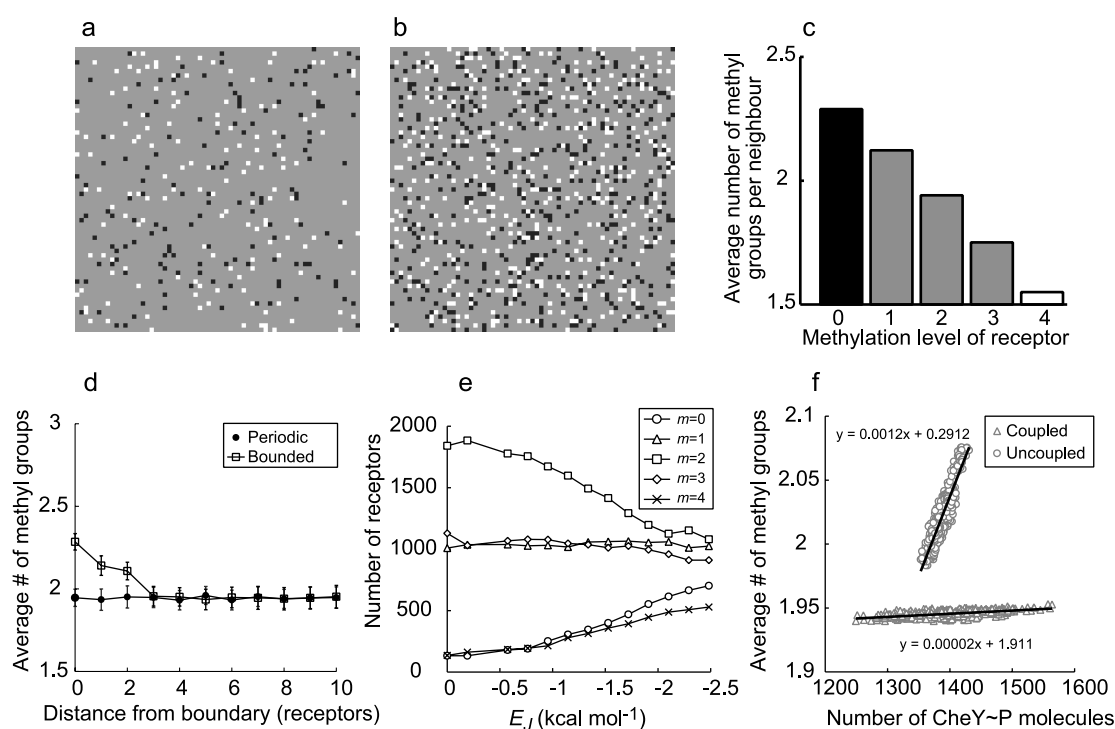


**Figure 6.** Patterns of methylation in the receptor lattice. The spatial distribution of methylation states is shown graphically for a  $65 \times 65$  square lattice with periodic boundaries (a) in the absence of coupling ( $E_J = 0.0$ ), and (b) with optimal coupling ( $E_J = -1.91 \text{ kcal mol}^{-1}$ ). Each small square in the image represents a single receptor complex in the lattice. White squares indicate a receptor with the highest level of methylation ( $m = 4$ ), black squares indicate receptors with the lowest level of methylation ( $m = 0$ ). Other receptors with intermediate levels of methylation ( $m = 1, 2, 3$ ) are shown in grey. (c) Nearest-neighbour influence on receptor methylation. For each of the five methylation states, the average number of methyl groups found on neighbouring receptors is plotted. The anticorrelation is significant (error bars are too small to be visible on this scale) and indicates that states with free energies  $\Delta G$  of opposite sign tend to lie next to one another. This tendency is due to the relationship between receptor activity and methylation reactions that is explained in the text. (d) If the periodic boundaries of (b) are replaced with finite boundaries, a mild but significant increase is observed in the average methylation level near the edge of the lattice (note that with periodic boundaries, the assignment of a boundary location is arbitrary). Error bars are frame-to-frame standard deviations of the mean value for receptors at the indicated distances. (e) The distribution of the total receptor population among the five methylation states as the coupling strength changes. A significant increase in the extreme methylation states ( $m = 0$  and  $m = 4$ ) is compensated by a proportional decrease in the average methylation state ( $m = 2$ ). (f) A further consequence of the coupling mechanism is found in the relationship between the average methylation level and CheY ~ P concentration. Each data point here represents a running average (ten seconds) over a 1500 seconds simulation of receptors without ligand addition. Linear fits to both data sets are also shown together with their equations.

However, the effect of methylation (and demethylation) feedback on the average activity of the system (that is, the slope of the fitted lines when the axes are inverted) is far greater in the coupled model: the effects of even very small changes in methylation are amplified, just as the effects of ligand binding.

## Discussion

Experimental and theoretical dissection of cooperative protein–protein interactions has a considerable history within biochemistry. The classical example is haemoglobin, whose sigmoid response to oxygen was first noted by Bohr in 1904. Work on haemoglobin led to the introduction of the Hill equation<sup>20</sup> and to two classical models of

allostery.<sup>21,22</sup> An interactive cycle of experimental and theoretical analysis then gradually uncovered the underlying mechanism of this and other allosteric interactions. Our analysis of the response of bacteria to the attractant aspartate follows in this spirit of seeking an adequate mechanistic model to account for the observed quantitative behaviour. Specifically, we have tested the possibility that allosteric interactions between adjacent receptors in a two-dimensional cluster could account for the shape and magnitude of the response of motile *E. coli* to changes in the attractant aspartate.

## Dose-response

In regard to the time-course of the chemotactic response, we compared our simulations to an

early study in which aspartate was ejected iontophoretically from a pipette positioned close to a tethered bacterium.<sup>16</sup> We found that our spatially extended StochSim model, with nearest-neighbour coupling, was able to reproduce the time-course of the response, including its pronounced undershoot. The latter phenomenon has been noted in numerous other swimming responses of bacteria, such as the response of *Rhodobacter* to changes in light intensity.<sup>23</sup> According to our analysis, the undershoot arises as a consequence of the lateral spread of inactive conformations away from each ligand-bound receptor. Inactive receptors are more likely to become methylated (by CheR), as part of the adaptation process, and their influence on total receptor activity remains after the primary stimulus has faded.

The inclusion of conformational spread in the simulation brings the amplitude of the attractant response closer to experimental observations, but significant differences remain. Because of the considerable variation in published values of chemotactic gain, some of which date back 30 years, we focused our attention on two recent estimates. The study of Sourjik & Berg<sup>17</sup> is especially relevant since it provides an estimate of the gain at the “front end” of the system, that is, the gain contributed by the receptor lattice independently of the flagellar motor. In this study the FRET signal between CheY ~ P and CheZ indicated a gain in CheY ~ P of approximately 35-fold over the change in receptor occupancy. In our best simulations, using an extended square lattice of receptors with optimal coupling, we achieved a front-end amplification of around tenfold. Although this falls significantly short of the FRET estimates, it should be noted that the comparison relies on an estimation of the apparent  $K_d$  for MeAsp binding to the Tar receptor, which is not a well-documented number. The Sourjik & Berg study<sup>17</sup> also revealed an unexpected effect of CheB on chemotactic gain, where mutants lacking CheB were found to have dramatically reduced sensitivity. One possible mechanism for the involvement of CheB in signal amplification was recently suggested by Barkai and colleagues,<sup>24</sup> but how this enzyme might be involved in signal amplification remains to be determined. Future experiments guided by detailed models should help to elucidate the underlying mechanisms.

The second estimate of gain came from the measurement of the changes in swimming of bacteria exposed to a sudden release of caged aspartate.<sup>18</sup> In order to compare our simulations with the results of this study we had to combine the predicted changes in CheY ~ P concentration with estimates of the effect these would have on the flagellar motor. The interaction of CheY ~ P with the flagellar motor is highly cooperative, with an estimated “Hill coefficient” (strictly a sensitivity coefficient) of 10.3.<sup>19</sup> Use of this value in our simulations led to an apparent gain that came close to the experimental record (see Figure 5).

There were, however, significant differences in the shape of the response curve. The slope of the coupled model’s response curve is steeper than the observed relation, rising rapidly to saturation. A more graded response, closer to the observed relation, can be obtained in our simulations if we assume that only a certain fraction of the total receptor population is clustered. The response of the whole system would then resemble a weighted average of the coupled and uncoupled responses (Figure 5, triangles), which could have a slope much closer to the observed logarithmic relation. This seems to be a reasonable assumption, in light of the observation that a minor fraction of chemoreceptors is found to be randomly distributed over the surface of the cell.<sup>25</sup> Another possible explanation for the discrepancy between the observed and simulated motor bias response is that our representation of the motor is too simplistic. We have used a simple Hill function to convert CheY ~ P concentrations from our simulation into motor bias. It is possible that interpretations using more realistic models of motor switching that have been recently proposed<sup>26–28</sup> could improve the fit to observed data.

Summarising our findings on the gain question, we first confirm the observation, made several times previously, that simple models in which the receptors are considered as independent entities are unable to match the amplification seen in the living bacteria. This is true even when the high cooperativity in the interaction between CheY ~ P and the motor is included. In agreement with Sourjik & Berg<sup>17</sup> we conclude that the principal source of unaccounted amplification is at the front end of the system, in or close to the cluster of receptors. Allosteric interactions between neighbouring receptors in this cluster, what we have termed “conformational spread”, are able to bring the gain much closer to experimentally observed values. We acknowledge that the fit is still not perfect, however, and that differences in both the form and magnitude of the response curve remain.

In considering these results, it is worth noting the recent suggestion by Bornhorst & Falke<sup>29</sup> that the simple two-state model of the type we have used here may not be adequate to explain the behaviour of all of the possible modification states of the Tar receptor. This argument is based on an analysis of *in vitro* kinase inhibition data obtained for engineered Tar receptor complexes in 16 different modification states.<sup>30</sup> A significant discrepancy between these new data and those of Borkovich *et al.*,<sup>31</sup> on which our activation probabilities (Table 2) are based, is in the sensitivity of fully modified receptors to ligand stimuli. One possible explanation for this discrepancy is that the microscopic ligand binding affinities (within the context of a two-state model; see Methods and Calculations) do vary with the receptor modification state.<sup>29</sup> We have not attempted to resolve this issue here as our focus has been to study the

effects of spatial interactions on the achievable amplification within the canonical two-state scheme. We note, however, that combinations of values do exist for the  $E_L$ ,  $E_M$  and  $E_J$  parameters of our model that make a population of fully modified receptors sensitive to ligand while maintaining a high  $K_{1/2}$  (T.S.S., unpublished results). Given our result that nearly wild-type levels of amplification are achievable through inter-receptor coupling without varying the affinities, it would seem that allowing for modest changes in ligand affinity with methylation could significantly improve the fit to the Hill-form of the *in vivo* data.

### Noise and response threshold

The incorporation of a coupling mechanism enhances the sensitivity of a population of chemotactic receptors over a range of background concentrations, and extends the dynamic range of their collective response. However, as can be seen in the traces of Figure 1, the steady-state level of noise increases with the coupling energy value  $E_J$ . The noise includes contributions due to the conformational flipping of receptors on a microsecond time scale; noise due to ligand binding on a millisecond time scale; and noise due to methylation reactions, which occur on a much slower time scale on the order of seconds; all of which are amplified in the coupled system. As the coupling strength increases, noise due to the slower methylation reactions dominates, producing regular oscillations. The presence of an adequate amount of noise is therefore essential for the conformational spread mechanism to act as an effective amplifying mechanism over a wide dynamic range. However, noise also degrades the quality of signal, so the threshold of detectable signals will also be affected by its magnitude. Ultimately, the amount of tolerable noise will depend on the filtering properties of the flagellar motor, the distribution of signals encountered in nature, as well as the costs and benefits associated with each signal. These issues merit further investigation, but are beyond the scope of the present study.

Nevertheless, it is important to note that because most experimentally documented responses measure averaged quantities, any amount of steady-state noise can in principle be reduced by repeated observations of motor switching or simultaneous observations of large populations of cells. The amplitude of the noise will decrease as the square root of the number of measurements (or the number of cells in a population). For the tethered cell experiments of Segall *et al.*<sup>16</sup> a typical impulse response was constructed by averaging over 100 records; the data for the swimming populations of Jasuja *et al.*<sup>18</sup> were constructed from the responses of more than 1000 bacteria. The noise incurred by our coupling mechanism (standard deviation  $\approx 12\%$ ) will have been negligible in these experiments.

### Methylation profiles of the receptor population

Adaptation of the *E. coli* chemotactic response is achieved by the enzymatic addition of methyl groups to four sites on each receptor chain. In our simulations we have allowed each receptor to have five possible free-energy states corresponding to 0, 1, 2, 3, or 4 methyl groups. Although the actual situation is far more complicated than this (with four sites per receptor chain, we could have  $2^8 = 256$  distinct methylation states per receptor dimer), it is nevertheless far closer to reality than the model with only a single methylation site described previously.<sup>13</sup> In the present study we found that enforcing a realistic kinetic mechanism for methylation reactions and introducing multiple methylation sites significantly alters the response of the system. In contrast to the simpler model of Duke & Bray,<sup>13</sup> there is not a single well-defined optimal coupling energy but rather a broad range over which the performance changes progressively. Although the maximum SNR was actually lower for receptors with four methylation sites than for receptors with one site, the receptor lattice in the former case was less sensitive to small changes in the coupling energy parameter. We therefore surmise that such an array would be more stable in the face of phenotypic variations and in that sense more robust than the receptors with a single site of methylation.

Population profiles of receptors with respect to the five methylation states were investigated and shown to be more diverse when the strength of coupling was higher, the increase in the extreme methylation states ( $m = 0$  and 4) being compensated by a proportional decrease in  $m = 2$  (Figure 6(e)). This phenomenon can be explained by the increased stability of the extreme states due to coupling. The stability of each methylation state is determined by how likely it is to be modified by CheR or CheB. However, the activities of these enzymes are themselves dependent on the activity of the receptor, since (in our simulations) CheR binds only to the inactive conformation and CheB only to the active conformation. In the uncoupled model, the extreme methylation states are highly unstable, because the receptor activities in these states are extremely biased (see greyed columns in Table 2). A fully methylated receptor, for example, will be almost exclusively in an active conformation, so that removal of its methyl groups (by CheB) will proceed at the maximum possible rate. With coupling, however, even the extreme methylation states can occupy a wide range of activation probabilities, depending on the number of active neighbours (Table 2). A fully methylated receptor in this environment will have a less-than-maximal activity, so removal of its methyl groups by CheB will occur at a slower rate.

It is therefore an inevitable consequence of the assumptions underlying our model that the methylation profiles of the receptors in a cluster with conformational coupling should differ from

those of an uncoupled system with the same activity. As mentioned, this difference should be characterised by increases in the extreme methylation states, compensated by a proportional decrease in receptors with two methyl groups, the most abundant methylation state in the absence of attractant. In principle it should be possible to test this prediction experimentally by rigorous characterisation of the methylation profiles.

The models we have developed for the behaviour of clusters of chemotaxis receptors have some of the properties of cellular automata. These are discrete dynamical systems whose behaviour is specified in terms of a local relation between otherwise identical units, or “cells”. Depending upon these local interactions, or rules, cellular automata often show the emergence of patterns, which can be very complex, and are usually impossible to predict.<sup>32</sup> Although most cellular automata that have been studied are deterministic, cellular automata can also be probabilistic, in that the state of each cell has a probability specified by its neighbours. A lattice of allosteric proteins such as the cluster of chemotactic receptors clearly fits this description and so one would expect the emergence of characteristic large-scale patterns. Indeed, we were able to detect the formation of spatial patterns of methylation within the coupled cluster of receptors. Specifically, we found that at steady-state, receptors with four methyl groups (fully methylated) and receptors with zero methyl groups (fully demethylated) tend to lie next to each other in the array (Figure 6(b) and (c)). There was also a higher level of methylation, on average, at the boundary of a lattice. These are only minimal degrees of order, but it is a direct consequence of assumptions made in the model, namely that (i) the activities of nearest-neighbours in the receptor cluster are coupled in a positive sense, and (ii) the activity of the adaptation enzymes CheR and CheB depend on the conformation of the substrate receptor. The spontaneous emergence of order within a stochastically fluctuating field of allosteric proteins is an intriguing and potentially important phenomenon. Indeed, the actual lattice could easily be more highly ordered, since other mechanisms, such as the localised action of the methyltransferase CheR,<sup>33</sup> have not been incorporated into our lattice model.

## Methods and Calculations

### Model of the chemotaxis network

Simulations were performed using the stochastic simulator StochSim 1.4,<sup>†</sup> a spatially extended version of the original StochSim program.<sup>11,35</sup> The reactions and rate constants of the model of the bacterial chemotaxis system were essentially as described,<sup>11</sup> except that some

or all of the receptor complexes were arranged in a regular two-dimensional lattice. All reaction mechanisms and rates are based on experimental findings in the literature, with the exception of methylation reactions which require a degree of tuning to account for the observed *in vivo* adaptation kinetics (see below). For clarity, we identify the crucial assumptions made in our model here.

First, receptors are assumed to be constantly undergoing a rapid transition between two conformational states, termed active and inactive, that determine the catalytic efficiency of the associated CheA kinase.<sup>31</sup> For simplicity, we further embrace the classic Monod–Wyman–Changeux model of allosteric transitions<sup>21</sup> in which the microscopic affinity to ligand of each of these two states, together with the fraction of time they are occupied, determine the observed macroscopic ligand binding affinities under various conditions. A scheme in which covalent modification affects only the rapid equilibrium between the two conformational states, but not the microscopic binding affinities, is sufficient to account for data obtained in the *in vitro* study of Borkovich *et al.*,<sup>31</sup> where both the ligand binding affinity and the effect of ligand binding on kinase activity were measured for receptors in various modification states.

A second important feature of our model is that the kinetic constants relating to methylation and demethylation have been tuned to account for the adaptation kinetics observed *in vivo*. Although these rates have been estimated on a number of occasions both *in vivo* and *in vitro*, there is still considerable uncertainty in the mechanisms and rate constants involved because both CheR and CheB have been found to interact with two distinct regions of the receptor (one that includes the substrate sites, and another at the C terminus of the receptor chain).<sup>36,37</sup> In the previously published parameter set on which our current model is based,<sup>11</sup> these reactions were approximated by a simple Michaelis–Menten type mechanism. To give the correct adaptation time-courses in that study, it was found that the catalytic rate constant of CheR and CheB had to be tuned to a value of  $0.819\text{ s}^{-1}$  and  $0.155\text{ s}^{-1}$ , respectively. The total rate of methylation by CheR in the model using this rate was at least several-fold higher than any previously reported rate.<sup>‡</sup> In this study, we found that in the model with optimal activity coupling, more moderate CheR and CheB rate constants of  $0.1\text{ s}^{-1}$  and  $0.02\text{ s}^{-1}$  give the best kinetic agreement to the observed response to both pulse stimuli (see Results) and step stimuli (data not shown). For the simplified model where receptors had only one methylation site, we found that it was necessary to modify the methylation kinetics and free-energy values of receptor conformational changes in order to maintain near-perfect adaptation. The parameters in this case were chosen so as to satisfy conditions for near-perfect adaptation that were obtained by analysis of the steady-state equations. Specifically, these conditions were: (1) the methyltransferase enzyme CheR operates at saturation; (2) the probability of activation of the unmethylated and ligand unbound receptor is small; (3) the free energy change upon methylation is large enough to keep adaptation error down, but not too large to have a response of reasonable size. The derivation of these conditions is given in Appendix A. Numerical values of methylation rate constants and free energy values that satisfy these

† Available for download from <http://www.zoo.cam.ac.uk/comp-cell/>

‡ See table of published rate constants at <http://www.zoo.cam.ac.uk/comp-cell/>

conditions are given in Table A1. Kinetic parameters of other reactions in the chemotaxis network were as in the full StochSim model.<sup>11</sup>

### Geometry and size of the receptor lattice

Receptors were arranged in three kinds of lattice: hexagonal (so that each receptor, or node, had three nearest neighbours), square (four neighbours), and trigonal (six neighbours). Lattice boundary conditions were either periodic, where each receptor had the same number of nearest neighbours, or finite, where receptors on boundaries had fewer neighbours and therefore received a weaker coupling interaction. In order to examine the effects of lattice size, we used square lattices with 4, 25, 100, 625, 2500, and 4225 receptors (in each simulation, in order to have the same total number of receptors, there were 625, 100, 25, 4, and 1 lattices, respectively). Each receptor had either four or one methylation sites.

### Calculation of free-energy and probability values

The activity of each receptor complex was determined by three free-energy inputs due to binding of a ligand molecule ( $E_L$ ), methylation ( $E_M$ ), and nearest neighbour interaction ( $E_j$ ).<sup>†</sup> For simplicity we assume that these energy inputs are independent of one another so that the free-energy difference  $\Delta G$  between the active and inactive form of the receptor is:

$$\Delta G = \Delta G_0 + lE_L + (m - m_0)E_M + (j - j_0)E_j \quad (1)$$

where  $l = 0, 1$  is the number of bound ligand molecules;  $m = 0, 1, 2, 3, 4$  is the number of methylated sites for the model with four methylation sites ( $m_0 = 2$ ) and  $m = 0, 1$  for the model with one methylation site ( $m_0 = 0$ );  $j = 0, \dots, c$  is the number of active nearest neighbours, where  $c = 3, 4, 6$  is the coordination number and  $j_0 = 3/2, 2, 3$  for the hexagonal, square, and trigonal geometries, respectively. The free energy “offset”  $\Delta G_0$  is zero for the model with four methylation sites. We assumed that the free-energy change for the conformation of an unliganded receptor complex with  $m_0$  methyl groups and  $j_0$  active neighbours is zero, giving an unbiased steady-state probability of activation of 0.5 in the model with four methylation sites. The choice of making  $m_0$  the unbiased methylation state is based on the observation *in vitro* that the ratio of activity for zero, half and fully methylated receptors is 0:0.5:1 in the absence of ligand stimuli.<sup>31</sup> Nullifying the coupling-energy input at  $j_0$  follows from the conformational-spread model,<sup>13</sup> which assumes that the effect of each neighbour in the same conformation is the exact opposite of each neighbour in the alternative conformation. An exception to equation (1) is the state with four methyl groups ( $m = 4$ ), which has an additional contribution of magnitude  $E_M$  in order to fulfil the requirement for perfect adaptation that the methylated state of the receptor complex be close to maximal activity.<sup>11</sup> States with  $j_0$  active neighbours, which have zero contribution of coupling energy, have  $\Delta G$  identical to the uncoupled model.

The estimate of the change in free energy  $E_L = 1.20$  kcal mol<sup>-1</sup> per binding of one ligand molecule was based on the observed  $K_d$  values for aspartate binding

to the Tar receptor, as described.<sup>11</sup> The magnitude of the change in free energy for the model with four methylation sites  $E_M = -1.20$  kcal mol<sup>-1</sup> per addition of one methyl group was assumed to be equal to that of  $E_L$ , but with the opposite sign. This implies that the addition of a single methyl group is sufficient to cancel out the effect of ligand binding to a receptor, and is consistent with the finding that the number of methyl groups on Tar increases by one following adaptation to saturating aspartate.<sup>38</sup> The value of the change in free energy  $E_j = -1.91$  kcal mol<sup>-1</sup> per addition of one active nearest neighbour in a square lattice of receptors with four methylation sites was estimated by optimisation of the output SNR (see Results). This value of  $E_j$  was used in all simulations with the square lattice unless stated otherwise. All absolute values for  $E_L$ ,  $E_M$  and  $E_j$  quoted here are calculated at  $T = 310$  K.

The difference in free energy  $\Delta G$  between the active and inactive states of the receptor complex is related to the probability  $p$  that the receptor is in the active state according to the following relationship:

$$p = \frac{1}{1 + e^{\Delta G/RT}} \quad (2)$$

where  $R = 1.9872$  cal mol<sup>-1</sup> K<sup>-1</sup> is the gas constant and  $T$  is the absolute temperature. We calculated  $\Delta G$  according to equation (1) for all permutations of the ligand-binding, methylation and neighbourhood states. Substituting the results into equation (2), we obtained the complete set of  $p$ -values for the coupled models that could then be used by the StochSim program. For the square lattice of receptors with four methylation sites, this set comprises 50 elements (Table 2). The  $p$ -values for the model with one methylation site can be calculated with values of free energy offset  $\Delta G_0$  and methylation energy  $E_M$  obtained in Appendix A and are shown in Table A1.

### Simulation protocols

Raw data were obtained as follows. The program StochSim was run a minimum of three times for each parameter set defining the configuration of the receptor lattice and the input stimulus. Initial conditions were generated by preliminary simulations that produced concentration sets defining the system adapted to the starting ligand concentration. The program produced time series data for the concentrations of different states of the receptor complex and other reactants in the system. The magnitudes of the attractant (aspartate) stimuli were in the range  $10^{-8}$ – $10^{-3}$  M and applied as either a prolonged step or a brief pulse (0.02–0.5 second duration).

### Data analysis

The raw time series from each simulation were imported into the spreadsheet program Microsoft Excel® and used to calculate the following quantities. Fitting of equations (3) and (5) was performed by the method of unweighted least-squares using the multi-purpose fitting program SpectFit by S. S. Andrews.<sup>‡</sup>

### Magnitude of the response

The output signal of the lattice was the peak drop  $\Delta y$

<sup>†</sup> The quantity that we call  $E_j$  here corresponds to four times the quantity called  $E_j$  by Duke & Bray<sup>13</sup> (see Appendix B).

<sup>‡</sup> <http://www.zoo.cam.ac.uk/comp-cell>

in the number of either active receptors or CheY ~ P molecules, depending on context. For ligand concentrations greater than 0.1  $\mu\text{M}$ , the peak drop was calculated as  $\Delta y = y_{\text{pre}} - y_{\text{min}}$ , where the prestimulus level,  $y_{\text{pre}}$ , was measured immediately before the stimulus application and the lowest value,  $y_{\text{min}}$ , was obtained as an average over 0.5 second following a 0.7 or 0.2 second delay after the stimulus application, or as a minimum over five seconds following stimulus. In this case calculations were done for each replicate run to obtain the mean and standard deviation. For ligand concentrations less than or equal to 0.1  $\mu\text{M}$  for the model with four methylation sites, and 1  $\mu\text{M}$  for the model with one methylation site, the data were more variable. For added smoothing the peak drop was calculated as  $\Delta y = y_{\text{st}} - y_{\text{min}}$ , where the steady-state adapted level  $y_{\text{st}}$  and the lowest value  $y_{\text{min}}$  were determined by fitting the adaptation portion of the time series to the exponential decaying function:

$$y = y_{\text{st}} - (y_{\text{st}} - y_{\text{min}})e^{-t/\tau} \quad (3)$$

where  $\tau$  is the characteristic adaptation time. For the fitting, in order to reduce the contribution to noise of variation between experiments while retaining thermal noise and noise due to ligand binding and methylation reactions, the time series from replicate runs were first aligned and averaged point-wise to obtain the “mean” time series for each lattice configuration. Standard deviations of fitted parameters were used to estimate standard deviations of the derived quantities.

#### Motor bias

The rotational bias of the flagellar motor  $mb$  is the proportion of time that it spends rotating in the counter-clockwise direction. It was calculated using the following phenomenological equation relating it to the CheY ~ P concentration  $y$ :<sup>39</sup>

$$mb = \left(1 + \frac{1 - mb_0}{mb_0} \left(\frac{y}{y_0}\right)^{n_H}\right)^{-1} \quad (4)$$

where  $mb_0 = 0.6$  is the steady-state motor bias,  $y_0$  is the steady-state CheY ~ P concentration with zero background attractant concentration, and  $n_H = 10.3$  is the Hill coefficient determined in experiments using optical methods in single cells.<sup>19</sup>

#### Sensitivity and gain

Simulated dose-response curves for the reduced aspartate concentration  $X = c/c_{0.5}$  and initial CheY ~ P response  $Y = 1 - \Delta y/y_{\text{pre}}$  or  $Y = 1 - \Delta y/y_{\text{st}}$  were fitted to a sigmoid equation:

$$Y = b + \frac{1 - b}{1 + (X/EC_{50})^h} \quad (5)$$

where  $c_{0.5} = \sqrt{K_d^a K_d^i}$  (apparent dissociation constant) gives 50% occupancy of the adapted receptor cluster with the steady-state activity 0.5,  $K_d^a$  and  $K_d^i$  are the dissociation constants for active and inactive conformations of receptor, respectively,  $b$  is the baseline,  $h$  is the Hill coefficient, and  $EC_{50}$  is the reduced ligand concentration that attains the half-maximal response  $Y = (1 + b)/2$ . With  $K_d^a = 12 \mu\text{M}$  and  $K_d^i = 1.7 \mu\text{M}$ ,<sup>11</sup> the apparent dissociation constant for aspartate is  $c_{0.5} = 4.6 \mu\text{M}$ . Occupancy of adapted receptors with the steady-state activity 0.5 is related to reduced concentration of aspar-

tate in the following way:

$$occ = \frac{X(X + \beta)}{X^2 + 2\beta X + 1} \quad (6)$$

where  $\beta = \left(\sqrt{(K_d^a/K_d^i)} + \sqrt{(K_d^i/K_d^a)}\right)/2$ . In Results, we report standard deviations for  $b$  and  $h$ . For  $EC_{50}$ , we report the 95% confidence interval.

In order to compare simulated dose-response curves with the experimental data, which were measured for MeAsp and plotted *versus* receptor occupancy in Figure 3(c) of Sourjik & Berg,<sup>17</sup> we recalculated their data to aspartate concentration that gives an equivalent receptor occupancy. The Hill equation for the initial CheY ~ P response, used by Sourjik & Berg,<sup>17</sup> is:

$$Y = 1 - \frac{occ^H}{occ^H + occ_{50}^H} \quad (7)$$

where  $occ$  is receptor occupancy in equation (6),  $occ_{50} = 0.014$  is occupancy that gives half-maximal response and  $H = 1.28$  is the Hill coefficient (parameters fitted by Sourjik & Berg<sup>17</sup>).

To quantify sensitivity amplification by the receptor lattice, we calculated chemotactic gain as either  $\Delta mb/\Delta occ$  or  $(\Delta y/y_{\text{pre}})/\Delta occ$  or  $(\Delta y/y_{\text{st}})/\Delta occ$ , where  $y$  is the number of either active receptors or CheY ~ P molecules. The change in receptor occupancy  $\Delta occ$  following the addition of a specified amount of ligand was calculated as the difference between occupancy averages over the pre- and post-stimulus periods.

#### Noise

For ligand concentrations greater than 0.1  $\mu\text{M}$  for the model with four methylation sites and 1  $\mu\text{M}$  for the model with one methylation site, noise in the lattice  $\eta$  was estimated as the variance around mean activity of receptors in the absence of ligand stimuli. For ligand concentrations less than or equal to 0.1  $\mu\text{M}$  and 1  $\mu\text{M}$  for models with four and one methylation sites, respectively,  $\eta$  was estimated as the mean squared displacement of the data from the fit obtained using equation (3). In this way we were able to give an aggregate measure of stochastic variation during the whole time of the response.

#### Signal-to-noise ratio

To quantify the signal transduction capability of a receptor lattice in the presence of internal noise that is caused by thermally induced fluctuations in molecular quantities and amplified by coupling between neighbouring receptors, we calculated the output SNR for the lattice stimulated by the step addition of aspartate with the peak drop in receptor activity  $\Delta y$  as the output signal:

$$\text{SNR} = \frac{(\Delta y)^2}{\eta} \quad (8)$$

#### Visualisation of methylation patterns

Spatial patterns of methylation were visualised by generating greyscale images in which receptor states with different number of methyl groups were labelled at different intensities. This was done using a custom-written Python program to process the receptor lattice snapshot data generated at regular intervals by the StochSim program during simulations. The data for

comparing the average number of methyl groups of nearest-neighbours and at the lattice boundaries (Figure 6(c) and (d)) were computed using custom-written Perl programs from snapshots taken at ten seconds intervals during long simulations (>5000 seconds) in the absence of ligand stimuli.

## Acknowledgements

We thank T. A. J. Duke for helpful discussions, S. S. Andrews for advice on data analysis and curve-fitting using the SpectFit program, and M. D. Levin for criticism of the manuscript. T.S.S. was supported by a Glaxo International Scholarship, an ORS Award from CVCP and a Bursary from the Cambridge Overseas Trust. This work was supported by grants from the MRC (G9810948) and NIGMS (GM64713) (to D.B.).

## References

- Geiger, B. & Bershadsky, A. (2001). Assembly and mechanosensory function of focal contacts. *Curr. Opin. Cell. Biol.* **13**, 584–592.
- Antonova, I., Arancio, O., Trillat, A. C., Wang, H. G., Zablow, L., Udo, H. *et al.* (2001). Rapid increase in clusters of presynaptic proteins at onset of long-lasting potentiation. *Science*, **294**, 1547–1550.
- Chan, C., George, A. J. & Stark, J. (2001). Cooperative enhancement of specificity in a lattice of T cell receptors. *Proc. Natl Acad. Sci. USA*, **98**, 5758–5763.
- Grakoui, A., Bromley, S. K., Sumen, C., Davis, M. M., Shaw, A. S., Allen, P. M. & Dustin, M. L. (1999). The immunological synapse: a molecular machine controlling T cell activation. *Science*, **285**, 221–227.
- Kennedy, M. B. (2000). Signal-processing machines at the postsynaptic density. *Science*, **290**, 750–754.
- Bren, A. & Eisenbach, M. (2000). How signals are heard during bacterial chemotaxis: protein-protein interactions in sensory signal propagation. *J. Bacteriol.* **182**, 6865–6873.
- Bourret, R. B. & Stock, A. M. (2002). Molecular information processing: lessons from bacterial chemotaxis. *J. Biol. Chem.* **277**, 9625–9628.
- Gestwicki, J. E. & Kiessling, L. L. (2002). Inter-receptor communication through arrays of bacterial chemoreceptors. *Nature*, **415**, 81–84.
- Ames, P., Studdert, C. A., Reiser, R. H. & Parkinson, J. S. (2002). Collaborative signaling by mixed chemoreceptor teams in *Escherichia coli*. *Proc. Natl Acad. Sci. USA*, **99**, 7060–7065.
- Bray, D. (2002). Bacterial chemotaxis and the question of gain. *Proc. Natl Acad. Sci. USA*, **99**, 7–9.
- Morton-Firth, C. J., Shimizu, T. S. & Bray, D. (1999). A free-energy-based stochastic simulation of the Tar receptor complex. *J. Mol. Biol.* **286**, 1059–1074.
- Shi, Y. & Duke, T. A. (1998). Cooperative model of bacterial sensing. *Phys. Rev. E*, **58**, 6399–6406.
- Duke, T. A. & Bray, D. (1999). Heightened sensitivity of a lattice of membrane receptors. *Proc. Natl Acad. Sci. USA*, **96**, 10104–10108.
- Domb, C. (1960). On the theory of cooperative phenomena in crystals. *Advan. Phys.* **9**, 149–244.
- Wang, W. & Wang, Z. D. (1997). Internal-noise-enhanced signal transduction in neuronal systems. *Phys. Rev. E*, **55**, 7379–7384.
- Segall, J. E., Block, S. M. & Berg, H. C. (1986). Temporal comparisons in bacterial chemotaxis. *Proc. Natl Acad. Sci. USA*, **83**, 8987–8991.
- Sourjik, V. & Berg, H. C. (2002). Receptor sensitivity in bacterial chemotaxis. *Proc. Natl Acad. Sci. USA*, **99**, 123–127.
- Jasuja, R., Lin, Y., Trentham, D. R. & Khan, S. (1999). Response tuning in bacterial chemotaxis. *Proc. Natl Acad. Sci. USA*, **96**, 11346–11351.
- Cluzel, P., Surette, M. & Leibler, S. (2000). An ultra-sensitive bacterial motor revealed by monitoring signaling proteins in single cells. *Science*, **287**, 1652–1655.
- Hill, A. V. (1913). The combinations of hemoglobin with oxygen and with carbon monoxide. *Biochem. J.* **7**, 471–480.
- Monod, J., Wyman, J. & Changeux, J. P. (1965). On the nature of allosteric transitions: a plausible model. *J. Mol. Biol.* **12**, 88–118.
- Koshland, D. E., Jr, Nemethy, G. & Filmer, D. (1966). Comparison of experimental binding data and theoretical models in proteins containing subunits. *Biochemistry*, **5**, 365–385.
- Berry, R. M. & Armitage, J. P. (2000). Response kinetics of tethered *Rhodobacter sphaeroides* to changes in light intensity. *Biophys. J.* **78**, 1207–1215.
- Barkai, N., Alon, U. & Leibler, S. (2001). Robust amplification in adaptive signal transduction networks. *C.R. Acad. Sci. Ser. IV-Phys. Astrophys.* **2**, 871–877.
- Maddock, J. R. & Shapiro, L. (1993). Polar location of the chemoreceptor complex in the *Escherichia coli* cell. *Science*, **259**, 1717–1723.
- Duke, T. A., Le Novère, N. & Bray, D. (2001). Conformational spread in a ring of proteins: a stochastic approach to allostery. *J. Mol. Biol.* **308**, 541–553.
- Scharf, B. E., Fahrner, K. A., Turner, L. & Berg, H. C. (1998). Control of direction of flagellar rotation in bacterial chemotaxis. *Proc. Natl Acad. Sci. USA*, **95**, 201–206.
- Turner, L., Samuel, A. D., Stern, A. S. & Berg, H. C. (1999). Temperature dependence of switching of the bacterial flagellar motor by the protein CheY(13D-K106YW). *Biophys. J.* **77**, 597–603.
- Bornhorst, J. A. & Falke, J. J. (2003). Quantitative analysis of aspartate receptor signaling complex reveals that the homogeneous two-state model is inadequate: development of a heterogeneous two-state model. *J. Mol. Biol.* **326**, 1597–1614.
- Bornhorst, J. A. & Falke, J. J. (2001). Evidence that both ligand binding and covalent adaptation drive a two-state equilibrium in the aspartate receptor signaling complex. *J. Gen. Physiol.* **118**, 693–710.
- Borkovich, K. A., Alex, L. A. & Simon, M. I. (1992). Attenuation of sensory receptor signaling by covalent modification. *Proc. Natl Acad. Sci. USA*, **89**, 6756–6760.
- Wolfram, S. (2002). *A New Kind of Science*, Wolfram Media, Champaign, IL.
- Levin, M. D., Shimizu, T. S. & Bray, D. (2002). Binding and diffusion of CheR molecules within a cluster of membrane receptors. *Biophys. J.* **82**, 1809–1817.
- Le Novère, N. & Shimizu, T. S. (2001). STOCHSIM: modelling of stochastic biomolecular processes. *Bioinformatics*, **17**, 575–576.
- Morton-Firth, C. J. & Bray, D. (1998). Predicting

- temporal fluctuations in an intracellular signalling pathway. *J. Theor. Biol.* **192**, 117–128.
36. Barnakov, A. N., Barnakova, L. A. & Hazelbauer, G. L. (1999). Efficient adaptational demethylation of chemoreceptors requires the same enzyme-docking site as efficient methylation. *Proc. Natl Acad. Sci. USA*, **96**, 10667–10672.
  37. Wu, J., Li, J., Li, G., Long, D. G. & Weis, R. M. (1996). The receptor binding site for the methyltransferase of bacterial chemotaxis is distinct from the sites of methylation. *Biochemistry*, **35**, 4984–4993.
  38. Stock, J. R. (1994). Adaptive responses in bacterial chemotaxis. In *Regulation of Cellular Signal Transduction Pathways by Desensitization and Amplification* (Sibley, D. R. & Houslay, M. D., eds), pp. 1–24, Wiley, New York.
  39. Bray, D. & Bourret, R. B. (1995). Computer analysis of the binding reactions leading to a transmembrane receptor-linked multiprotein complex involved in bacterial chemotaxis. *Mol. Biol. Cell*, **6**, 1367–1380.
  40. Yi, T. M., Huang, Y., Simon, M. I. & Doyle, J. (2000). Robust perfect adaptation in bacterial chemotaxis through integral feedback control. *Proc. Natl Acad. Sci. USA*, **97**, 4649–4653.
  41. Barkai, N. & Leibler, S. (1997). Robustness in simple biochemical networks. *Nature*, **387**, 913–917.
  42. Mello, B. A. & Tu, Y. (2003). Perfect and near perfect adaptation in a model of bacterial chemotaxis. *Biophys. J.* **84**, 2943–2956.

## Appendix A

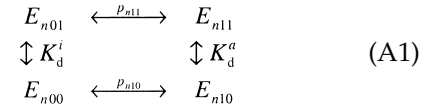
To obtain the conditions for near-perfect adaptation in the model with one methylation site, we have used the strategy of eliminating from the steady-state equations all variables that depend on any particular methylation state of receptor and ligand concentration. If the resulting system of equations can be resolved, the solution at steady-state is the same for any ligand concentration (perfect adaptation). This strategy follows Yi *et al.*,<sup>40</sup> who derived an integral control equation for receptor activity from Barkai & Leibler's equations,<sup>41</sup> and Mello & Tu<sup>42</sup> who derived a complete set of perfect adaptation conditions for phosphorylated CheY. Here, we considered the front-end of the chemotaxis network with the total receptor activity as the adapting variable. The effect of the downstream phosphorylation reactions on adaptation is considered by Mello & Tu<sup>42</sup> and does not depend on the number of methylation sites.

We denote receptor by symbol  $E_{nj\bar{k}}$  where subscripts  $n, j, \bar{k}$  have the following meaning:  $n = 0, 1$  signifies the number of methylated sites,  $j = 0$  and  $j = 1$  signify inactive and active conformation, respectively, and  $\bar{k} = 0$  and  $\bar{k} = 1$  signify ligand unbound and bound state, respectively. For example,  $E_{010}$  signifies unmethylated and ligand-unbound receptor in an active conformation.

### Receptor conformational changes

Ligand binding and conformational change of receptor occur on much faster time scales than all

other reactions and are treated as rapid equilibria. Receptor species in any methylation state  $E_{0j\bar{k}}$  and  $E_{1j\bar{k}}$  are related to each other through conservation of mass and free energy:



where  $p_{n1k} = E_{n1k}/(E_{n1k} + E_{n0k})$  are fractions of active receptor having  $n$  methylated sites and ligand binding state  $k$  and  $K_d^i$  and  $K_d^a$  are ligand dissociation constants for inactive and active receptor, respectively. We assumed that these microscopic dissociation constants (i.e. the  $K_d$ s for the rapidly changing receptor conformations) are independent of receptor methylation state. For the thermodynamic cycle of receptor species in equation (A1), the change of free energy is zero and thus any of the four receptor species with  $n$  methylated sites can be calculated given the total ligand concentration  $L$ , the total receptor concentration with  $n$  methylated sites  $E_{(n)} \equiv E_{nj\bar{k}} = E_{n00} + E_{n10} + E_{n11} + E_{n01}$ , dissociation constants  $K_d^i, K_d^a$ , and the probability of activation of unliganded receptor  $p_{n10}$ . For example, the concentration of inactive and ligand bound receptor with  $n$  methylated sites is:

$$E_{n01} = E_{(n)} \frac{\frac{L}{K_d^i}}{1 + \frac{L}{K_{d,n}^{\text{eff}}}} (1 - p_{n10}) \quad (\text{A2})$$

where the effective dissociation constant  $K_{d,n}^{\text{eff}}$  for  $n$ -methylated and non-adapted receptor species is given by:

$$\frac{1}{K_{d,n}^{\text{eff}}} = \frac{1 - p_{n10}}{K_d^i} + \frac{p_{n10}}{K_d^a} \quad (\text{A3})$$

Fractions of active receptor (probabilities of activation) can be expressed in terms of  $p_{010}$ ,  $e_0$  and dissociation constants as follows:

$$\begin{aligned} p_{011} &= \frac{1}{1 + \frac{K_d^a}{K_d^i} \frac{1 - p_{010}}{p_{010}}}, \\ p_{110} &= \frac{1}{1 + e_0 \frac{1 - p_{010}}{p_{010}}}, \\ p_{111} &= \frac{1}{1 + e_0 \frac{K_d^a}{K_d^i} \frac{1 - p_{010}}{p_{010}}} \end{aligned} \quad (\text{A4})$$

where the parameter  $e_0 = \exp(E_M/RT) < 1$  and  $E_M$  is the change of free energy upon methylation.

Response size is defined as the overall drop in receptor activity immediately after stimulus and is determined by the difference in activation

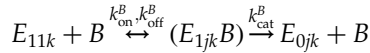
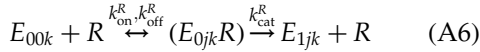
probabilities of ligand-bound and unbound methylated species,  $\Delta p_{(1)} = p_{110} - p_{111}$ , and unmethylated species,  $\Delta p_{(0)} = p_{010} - p_{011}$ . Using the expressions for probabilities in equations (A4) we obtain:

$$\Delta p_{(1)} = \frac{\frac{e_0}{p_{010}} \left( \frac{K_d^a}{K_d^i} - 1 \right) (1 - p_{010})}{\left( 1 + \frac{e_0}{p_{010}} (1 - p_{010}) \right) \left( 1 + \frac{e_0}{p_{010}} \frac{K_d^a}{K_d^i} (1 - p_{010}) \right)},$$

$$\Delta p_{(0)} = \frac{p_{010} (1 - p_{010}) \left( \frac{K_d^a}{K_d^i} - 1 \right)}{\left( p_{010} + \frac{K_d^a}{K_d^i} (1 - p_{010}) \right)} \quad (\text{A5})$$

### Methylation reactions

Methylation reactions occur on a slower time-scale. Assuming that the methyltransferase CheR binds only inactive receptor and the methyl-esterase CheB binds only active receptor, we have the following reactions:



where  $R$  and  $B$  denote the concentration of free CheR and CheB enzymes and the  $k$ s are rate constants of elementary uni- and bi-molecular reactions. CheB here refers to amount of active CheB species that demethylates active receptors, since we ignore the phosphorylation part of the signalling pathway. Notice that all receptor species including those bound to CheR and CheB can be either ligand-bound or unbound and either active or inactive because of the difference in time scales. Using the principle of mass-action, we write differential equations describing methylation dynamics as:

$$\frac{d\{E_{(0)}R\}}{dt} = k_{\text{on}}^R (E_{000} + E_{001})R - (k_{\text{off}}^R + k_{\text{cat}}^R) \{E_{(0)}R\} \quad (\text{A7})$$

$$\frac{d\{E_{(1)}B\}}{dt} = k_{\text{on}}^B (E_{110} + E_{111})B - (k_{\text{off}}^B + k_{\text{cat}}^B) \{E_{(1)}B\}$$

$$\frac{dE_{(1)}}{dt} = k_{\text{cat}}^R \{E_{(0)}R\} + k_{\text{off}}^B \{E_{(1)}B\} - k_{\text{on}}^B (E_{110} + E_{111})B$$

$$\frac{dE_{(0)}}{dt} = k_{\text{off}}^R \{E_{(0)}R\} + k_{\text{cat}}^B \{E_{(1)}B\} - k_{\text{on}}^R (E_{000} + E_{001})R$$

Sums of receptor species  $E_{000} + E_{001}$  and  $E_{110} + E_{111}$  can be related to  $E_{(0)}$  and  $E_{(1)}$  using probabilities in equation (A4) in a way similar to equation (A2)

and are calculated as follows:

$$E_{n00} + E_{n01} = E_{(n)} \frac{1 + \frac{L}{K_d^i}}{1 + \frac{L}{K_{d,n}^{\text{eff}}}} (1 - p_{n10}),$$

$$E_{n10} + E_{n11} = E_{(n)} \frac{1 + \frac{L}{K_d^a}}{1 + \frac{L}{K_{d,n}^{\text{eff}}}} p_{n10} \quad (\text{A8})$$

Fractions on the right-hand sides of equations (A8) are by definition related to the total fraction of active receptors in methylation state  $n$  (without regard for their ligand binding state):

$$P_{n1k} = \frac{1 + \frac{L}{K_d^a}}{1 + \frac{L}{K_{d,n}^{\text{eff}}}} p_{n10} \quad (\text{A9})$$

Using equations (A8) and (A9) and making a quasi-steady-state assumption for enzyme-substrate binding in the first two of equation (A7), we obtain:

$$\{E_{(0)}R\} = \frac{E_{(0)}R}{K_M^R} (1 - P_{01k}), \quad \{E_{(1)}B\} = \frac{E_{(1)}B}{K_M^B} P_{11k} \quad (\text{A10})$$

where Michaelis constants are defined as:

$$K_M^R = \frac{k_{\text{off}}^R + k_{\text{cat}}^R}{k_{\text{on}}^R}, \quad K_M^B = \frac{k_{\text{off}}^B + k_{\text{cat}}^B}{k_{\text{on}}^B} \quad (\text{A11})$$

### Steady-state equations

The last two of equation (A7) produce an identical equation for the overall methylation flux at steady state:

$$k_{\text{cat}}^R \frac{E_{(0)}R}{K_M^R} (1 - P_{01k}) = k_{\text{cat}}^B \frac{E_{(1)}B}{K_M^B} P_{11k} \quad (\text{A12})$$

The methylation flux in equation (A12) has to be complemented with conservation equations for total CheR, CheB, and receptor:

$$R_{\text{tot}} = R + \{E_{(0)}R\}, \quad B_{\text{tot}} = B + \{E_{(1)}B\},$$

$$E_{\text{tot}} = E_{(0)} + E_{(1)} + \{E_{(0)}R\} + \{E_{(1)}B\} \quad (\text{A13})$$

Using equations (A10) we can rewrite equations (A13) as:

$$R_{\text{tot}} = R \left( 1 + \frac{E_{(0)}}{K_M^R} (1 - P_{01k}) \right),$$

$$B_{\text{tot}} = B \left( 1 + \frac{E_{(1)}}{K_M^B} P_{11k} \right) \quad (\text{A14})$$

$$E_{\text{tot}} = E_{(0)} \left( 1 + \frac{R}{K_M^R} (1 - P_{01k}) \right) + E_{(1)} \left( 1 + \frac{B}{K_M^B} P_{11k} \right)$$

Our strategy is now to rearrange equations (A12) and (A14) so that these four steady-state equations are “global”, i.e. do not depend on ligand concentration or variables in any particular methylation state, either  $E_{(0)}$  or  $E_{(1)}$ , but on four global variables corresponding to concentrations of free enzymes  $R$  and  $B$ , total free receptor  $E_{\text{tot}}^f = E_{(0)} + E_{(1)}$  and total free active receptor  $E_{\text{tot}}^{fa} = P_{01k}E_{(0)} + P_{11k}E_{(1)}$ . As a result we have:

$$k_{\text{cat}}^B B \frac{E_{\text{tot}}^{fa}}{K_M^B} = \left( k_{\text{cat}}^R + k_{\text{cat}}^B \frac{BK_M^R}{RK_M^B} \frac{P_{01k}}{1 - P_{01k}} \right) \times \left[ \frac{E_{(0)}R}{K_M^R} (1 - P_{01k}) \right] \quad (\text{A15})$$

$$R_{\text{tot}} = R + \left[ \frac{E_{(0)}R}{K_M^R} (1 - P_{01k}) \right]$$

$$B_{\text{tot}} = B \left( 1 + \frac{E_{\text{tot}}^{fa}}{K_M^B} \right) - \frac{BK_M^R}{RK_M^B} \frac{P_{01k}}{1 - P_{01k}} \times \left[ \frac{E_{(0)}R}{K_M^R} (1 - P_{01k}) \right]$$

$$E_{\text{tot}} = E_{\text{tot}}^f + B \frac{E_{\text{tot}}^{fa}}{K_M^B} + \left( 1 - \frac{BK_M^R}{RK_M^B} \frac{P_{01k}}{1 - P_{01k}} \right) \times \left[ \frac{E_{(0)}R}{K_M^R} (1 - P_{01k}) \right]$$

We also have to consider total receptor activity  $E_{\text{tot}}^a = P_{01k}(E_{(0)} + \{E_{(0)}R\}) + P_{11k}(E_{(1)} + \{E_{(1)}B\})$ :

$$E_{\text{tot}}^a = E_{\text{tot}}^{fa} \left( 1 + \frac{B}{K_M^B} P_{11k} \right) + P_{01k} \left( 1 - \frac{BK_M^R}{RK_M^B} \frac{P_{11k}}{1 - P_{01k}} \right) \times \left[ \frac{E_{(0)}R}{K_M^R} (1 - P_{01k}) \right] \quad (\text{A16})$$

### Conditions for near-perfect adaptation

We see now that equations (A15) and (A16) depend on ligand concentration  $L$  (through activity fractions  $P_{n1k}$ , see equation (A9)) and zero-methylation state  $E_{(0)}$  (terms in square brackets). Thus the steady-state equations cannot be made global, which precludes perfect adaptation. However, we can make these equations approximately global for near-perfect adaptation by adjusting biochemical parameters in the following way.

As is seen in equation (A9), dependence of  $P_{01k}$  and  $P_{11k}$  on  $L$  can be eliminated (their contribution made numerically small) by making these fractions either close to 0 by letting  $p_{n10} \rightarrow 0$  or close to 1 by letting  $p_{n10} \rightarrow 1$  (which reduces the difference between  $K_d^a$  and  $K_{d,n}^{\text{eff}}$ ). However, if  $p_{n10} \rightarrow 0$  or

$p_{n10} \rightarrow 1$  for both  $n = 0$  and  $n = 1$ , the initial response to ligand will vanish as can be seen from equation (A5). To make the response size larger, we should have either  $p_{010} \rightarrow 1$  and  $p_{110} \rightarrow 0$ , which is impossible by assumption that methylation increases probability of activation ( $e_0 < 1$ ), or  $p_{010} \rightarrow 0$  (small probability of activation of virgin receptor) and  $p_{110} \rightarrow 1$ . The latter is achieved with large absolute value of the methylation energy,  $e_0 \rightarrow 0$  such that  $e_0 = O(p_{010})$  (if  $e_0 = o(p_{010})$  the response size again vanishes). Dependence of the steady-state equations on  $E_{(0)}$  can be eliminated by making constant the terms in square brackets, which with the help of equation (A10) are identified as the concentration of CheR enzyme–substrate complex  $\{E_{(0)}R\}$ . This can be achieved by assuming saturation of CheR. (In fact,  $p_{010} \rightarrow 0$  is also needed to maintain CheR saturation so that the substrate,  $E_{(0)}$ , is in excess to the enzyme CheR.)

However, the effect of the above manipulations on adaptation error can be either synergistic or antagonistic and is either amplified or attenuated by the kinetics and the steady state of the system. As a result, the near-perfect adaptation requires carefully chosen parameter values. In particular, as mentioned above, there is a trade-off between increasing the response size (larger  $e_0$  to maximise  $\Delta p_{(1)}$ ) and eliminating the contribution of  $L$  terms (smaller  $e_0$  to have  $p_{110} \rightarrow 1$ ).

We found that near-perfect adaptation can nevertheless be achieved without saturating CheR, in which case parameters are such that variation in  $\{E_{(0)}R\}$  has only a small effect on the steady-state solution. But this has the consequence of increasing the effect of variation of  $P_{01k}$  and  $P_{11k}$ , as functions of ligand concentration  $L$ . To eliminate this effect,  $p_{010}$  has to be made several orders of magnitude smaller than if CheR were saturated. However, a very small  $p_{010}$  (on the order of  $10^{-10}$ ) is not realistic, since this implies a very large free energy change  $\Delta G$  of receptor activation, which is inconsistent with the observed energetics of conformational changes in proteins. Furthermore, in this scheme, adaptation error can be kept small only if the steady-state activity is much smaller than 0.5.

### Parameter values

Values of kinetic parameters and free energy of receptor activation that satisfy the above conditions are given in Table A1 below. Free energies were calculated as in Methods and Calculations with probability of activation of unliganded and unmethylated receptor  $p_{010}$  set to  $5.71 \times 10^{-4}$  (corresponding to the free energy change  $\Delta G_0 = 4.6$  kcal mol $^{-1}$ ), and methylation energy parameter  $e_0$  set to  $4.54 \times 10^{-5}$  (corresponding to methylation energy  $E_M = -6.16$  kcal mol $^{-1}$ ). With these values, steady-state receptor activity is around 0.5 and adaptation error is around 3%, and CheR is saturated with the Michaelis constant 0.013  $\mu\text{M}$ .

**Table A1.** Parameter values for the model with one methylation site

		$k_f$	$k_r$
Demethylation	$E_1^a + B_p \leftrightarrow E_1 B_p$	$4.8 \times 10^5 \text{ M}^{-1} \text{ s}^{-1}$	$17.5 \text{ s}^{-1}$
	$E_1 B_p \rightarrow E_0 + B_p$	$3.73 \text{ s}^{-1}$	0
Methylation	$E_0^i + R \leftrightarrow E_0 R$	$10^8 \text{ M}^{-1} \text{ s}^{-1}$	$0.05 \text{ s}^{-1}$
	$E_0 R \rightarrow E_1 + R$	$1.25 \text{ s}^{-1}$	0
$p$	Unmethylated	Ligand unbound	Ligand bound
$\Delta G$ (kcal mol <sup>-1</sup> )	Unmethylated	0.0	0.0
$p$	Methylated	4.6	5.8
$\Delta G$ (kcal mol <sup>-1</sup> )	Methylated	0.926	0.641
		-1.56	-0.36

$E$  represents receptor complex, superscripts  $i$  and  $a$  signify inactive and active receptor, subscripts 0 and 1 signify unmethylated and methylated receptor. Receptors without a superscript can be either active or inactive.

## Appendix B

The definition of  $E_j$  by Duke & Bray<sup>13</sup> was analogous to the interaction energy  $\varepsilon$  in the Ising model, which appears in the coupling term  $\varepsilon \sum_{\langle i,j \rangle} s_i s_j$  of the Ising energy expression. The sum over  $\langle i,j \rangle$  here covers all nearest-neighbour pairs, and the variables  $s_i$  and  $s_j$  indicate the state of site  $i$  and each of its nearest neighbours ( $j = 1, 2, 3, 4$

for a square lattice). In the Ising model, each state can take the value of 1 or -1 (analogous to active or inactive state of the receptor complex, respectively), so the absolute energy difference between the case where  $s_i = 1$  and  $s_i = -1$  is given by  $2\varepsilon \sum_j s_j$ . The factor  $\sum_j s_j = -4, -2, 0, 2, 4$  for 0, 1, 2, 3, 4 active neighbours, whereas the factor  $(j - j_0)$  in equation (1) takes the values -2, -1, 0, 1, 2. Therefore,  $E_j$  in equation (1) maps to  $4\varepsilon$ .

*Edited by I. B. Holland*

(Received 14 January 2003; received in revised form 21 March 2003; accepted 26 March 2003)